

Water on silicon (001): *C* defects and initial steps of surface oxidation

O. Warschkow,¹ S. R. Schofield,² N. A. Marks,¹ M. W. Radny,² P. V. Smith,² and D. R. McKenzie¹
¹Centre for Quantum Computer Technology, School of Physics, The University of Sydney, Sydney NSW 2006, Australia
²School of Mathematical and Physical Sciences, The University of Newcastle, Callaghan NSW 2308, Australia

(Received 16 March 2008; published 22 May 2008)

The recent literature has now firmly attributed the common *C* defect on the Si(001) surface to the dissociative adsorption of water. This work, by examining the dynamical properties of the *C* defect at elevated temperatures (≈ 450 K), establishes the missing mechanistic link between dissociative water adsorption and wet surface oxidation. Scanning tunneling microscopy and density functional theory in combination reveal in detail the various paths by which a water molecule breaks apart on the surface and inserts oxygen atoms into the surface.

DOI: 10.1103/PhysRevB.77.201305

PACS number(s): 68.43.Bc, 68.37.Ef, 68.47.Fg

The reaction of water with the Si(001) surface is technologically relevant in the fabrication of ultrathin silicon-oxide gate dielectrics. As such, the atomic-scale processes of the $\text{H}_2\text{O}:\text{Si}(001)$ reaction system have received considerable attention. It is well established^{1–8} that H_2O adsorbs dissociatively at room temperature, which produces OH and H fragments bonded to the Si-Si dimers of the surface. Scanning tunneling microscopy (STM) experiments^{2,4,8} have identified two types of surface features that are correlated with H_2O exposure; one has the appearance of a single asymmetric dark dimer; the other is familiar as the *C* defect,⁹ a Si(001) surface impurity commonly encountered in STM experiments. As outlined in Figs. 1(a)–1(c), these two features are now understood^{4–6,8} to correspond to the same- and adjacent-dimer H+OH species, respectively. At higher temperatures, further dissociation becomes possible with infrared spectroscopy³ showing that a single-dimer H-Si-O-Si-H species [Fig. 1(d)] is formed at 575–675 K. This species is an important intermediate in the formation of silicon dioxide as it contains an oxygen atom inserted into a Si-Si surface dimer. For the special case of a chlorine-covered silicon surface, a recent STM study¹⁰ revealed a correlation between *C* defects observed at room temperature and the number of Si-O-Si dimers formed after anneal. With this Rapid Communication, we resolve the missing chemical mechanism by which these oxygen-inserted species are formed. We report detailed STM experiments at elevated temperature and density functional theory (DFT) calculations to reveal how *C* defects (H+OH) break apart into three types of oxygen-inserted 2H+O species. The routes taken to form these species highlight the importance of interdimer reactions absent in many previous models of H_2O -induced silicon surface oxidation.^{11–14}

Density functional theory calculations were performed using the GAUSSIAN03 software¹⁵ and a four-dimer $\text{Si}_{27}\text{H}_{24}$ cluster representation of the Si(001) surface. Formation energies were calculated using B3LYP hybrid exact exchange, a composite Gaussian-type basis set, and additional corrective terms to account for finite cluster size, finite basis set size, and vibrational zero-point effects.¹⁶ Formation energies calculated by using this method for various intermediates and transition states of room-temperature H_2O adsorption and/or dissociation [given in Fig. 1(a)] agree well with those of previous works.^{5,6} Specifically, the H_2O molecular adsorp-

tion species (at -0.51 eV), the dissociated adjacent-dimer H+OH (-2.32 eV), and the same-dimer H+OH species (-2.58 eV) increase in thermodynamic stability. The calculated activation energies (E_A) for dissociation of molecularly adsorbed H_2O into same-dimer and adjacent-dimer H+OH are very similar (0.28 and 0.26 eV, respectively). This also matches earlier calculations⁶ and agrees with the experimental finding^{2,5,8} that both structures [as asymmetric features and *C* defects; Figs. 1(b) and 1(c)] are formed at room temperature.

In order to understand how these two H+OH species dissociate at elevated temperatures, we first consider an OH fragment in isolation and categorize several plausible onward reactions [Figs. 2(a)–2(d)]. We find that OH dissociation by interdimer H shift [Fig. 2(a); transfer of hydrogen to an adjacent dimer] with an activation energy of $E_A=1.67$ eV is kinetically preferred over OH dissociation by intradimer H shift [Fig. 2(b); $E_A=2.31$ eV] and insertion of the complete OH fragment into a Si-Si dimer [Fig. 2(c); $E_A=1.81$ eV].

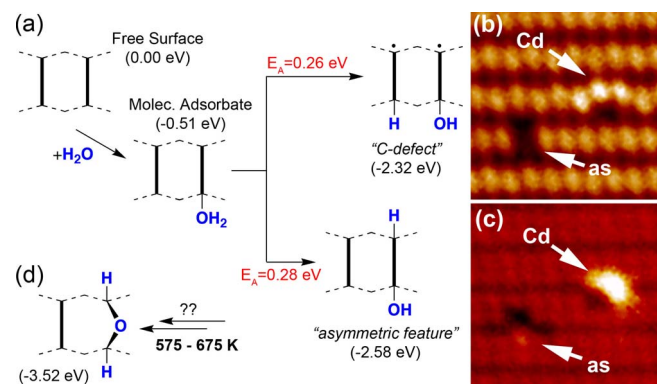


FIG. 1. (Color online) (a) Schematic valence structure diagrams of the room-temperature adsorption and dissociation of H_2O on Si(001) leading to the adjacent- and same-dimer OH+H species. These species are experimentally observed as *C* defects (Cd) and asymmetric (as) features in (b) filled- and (c) empty-state STM images. (d) The single-dimer H-Si-O-Si-H species reported (Ref. 3) to form in the 575–675 K temperature range. Our schematic structure diagrams assume Si atoms at the vertices and use bold vertical lines to indicate Si-Si surface dimers and dotted lines for the backbonds.

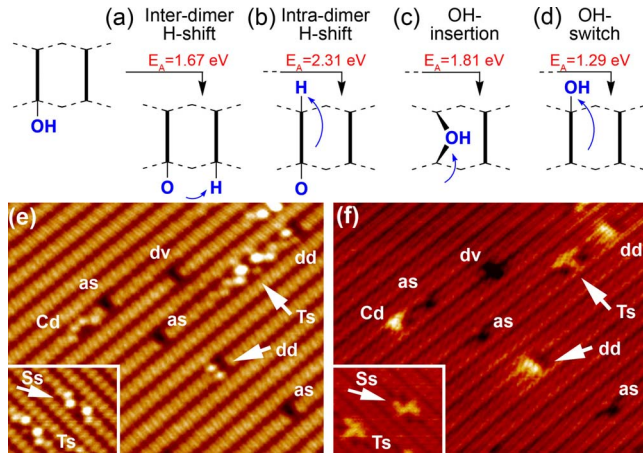


FIG. 2. (Color online) [(a)–(d)] Schematic outline of plausible onward reactions of an OH fragment on Si(001) and calculated activation energies (E_A). (e) Filled- and (f) empty-state STM images of an H_2O -exposed Si(001) surface *in situ* heated to approximately 450 K. Three features—T shaped (Ts), S shaped (Ss), and double dot (dd)—arising from C-defect dissociation are indicated by arrows. A dimer-vacancy (dv) defect is also seen, which is distinct from the asymmetric (as) feature in the empty-state image.

This finding is in contrast to the literature,^{11–14} which has advanced the latter reaction (OH insertion) as the primary route of wet surface oxidation without considering the inter-dimer H shift as a possibility. Our discovery of this process as a reaction channel with a smaller activation energy suggests that OH dissociation and surface oxidation commence at lower temperatures and by a dramatically different route than previously thought. A fourth reaction, the OH switch [Fig. 2(d); transfer of the OH fragment from one dimer end to another] presents a much lower activation barrier (1.29 eV) and is therefore more easily activated than the inter-dimer H shift. Note, however, that the initial and final structures of the OH switch are equivalent; thus, we should expect the switch to reversibly occur many times before the OH fragment dissociates via the inter-dimer H shift.

The discussion in the previous paragraph considered an isolated OH; however, we find that the same process occurs for a dissociated H_2O molecule (i.e., $\text{HO}+\text{H}$) with activation energies slightly changed due to the presence of the second hydrogen atom. Okano and Oshiyama⁵ previously ascribed OH-switch reactions to C-defect transitions seen in experiment.¹⁷ We additionally observe that inter-dimer H shift is the rate-determining step of C-defect dissociation and wet silicon surface oxidation. We have been able to directly image such transitions in scanning tunneling microscopy experiments conducted on a H_2O -exposed Si(001) surface that is resistively heated *in situ* to approximately 450 ± 50 K. Atomic resolution images were obtained using an Omicron variable-temperature STM operating under ultrahigh vacuum conditions at a base pressure of 2×10^{-11} mbar.¹⁸ All images shown herein were acquired in pairs by using tip-sample biases of +2 V (empty state image) and –2 V (filled state), a current of 0.3 nA, and at a rate of approximately one image pair every 3 min over a period of several hours. In the sequence of images, C defects and asymmetric features were

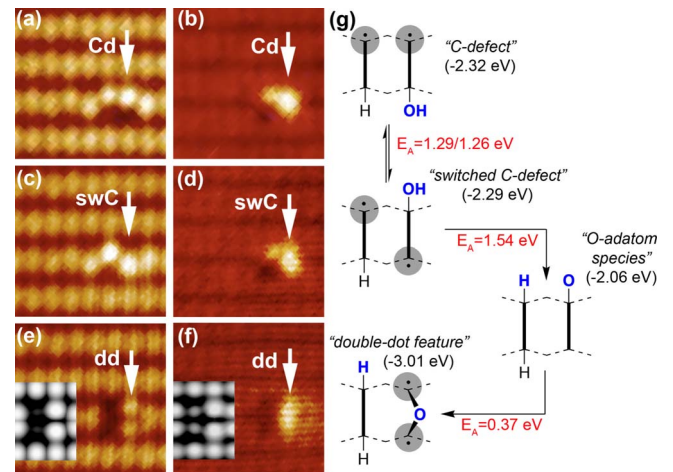


FIG. 3. (Color online) Sequence of STM images in [(a), (c), and (e)] filled state and [(b), (d), and (f)] empty state, showing a C defect (labeled Cd) change into a switched C defect (swC), which in turn dissociates into a double-dot feature (dd). (g) Schematic valence diagram of the reaction steps revealed in these images. Gray shading indicates the threefold bonded silicon sites that typically image bright in STM.

seen to undergo a variety of transformations. A representative large-scale image in filled and empty states is shown in Figs. 2(e) and 2(f): C defects and asymmetric features are still present on the surface; two new features—the *double-dot* and the *T-shaped* feature—are indicated by arrows. A third, less-common *S-shaped* feature is presented in an inset of Figs. 2(e) and 2(f). All three originate from C defects by inter-dimer OH dissociation.

The prototypical dissociation reaction of a C defect proceeds, as shown in Fig. 3. This sequence of three images each for filled and empty states shows a C defect [Figs. 3(a) and 3(b)] change into a *double-dot feature* [Figs. 3(e) and 3(f)] via an intermediate feature [Figs. 3(c) and 3(d)] that we refer to as a *switched C defect*. The chemical processes that are revealed in these images are outlined alongside in Fig. 3(g). Following Refs. 4 and 8, the orientation of the C defect in Figs. 3(a) and 3(b) is as shown in the adjacent schematic with H and OH fragments located on the lower left- and right-hand dimer ends, respectively. The threefold bonded silicon atoms on the upper dimer ends present single dangling bonds that typically image bright in STM. We have highlighted such sites with gray shading in our valence schematics to facilitate comparison with experiment. In the switched C defect [Figs. 3(c) and 3(d)], the dangling bond of the OH dimer (white arrow) has shifted to the lower dimer end; this is best seen in the filled-state image. In other words, an OH-switch reaction has taken place. In the next set of images [Figs. 3(e) and 3(f)], the switched C defect has changed into a double-dot feature. This occurs via the postulated inter-dimer H-shift reaction that produces in the first instance [Fig. 3(g)] a single-bonded oxygen adatom and a H-Si-Si-H monohydride dimer. This adatom species is metastable relative to either form of the C defect and short lived, being able to considerably stabilize (a further 1 eV) by inserting the oxygen atom into the Si-Si dimer bond. The two dangling bonds of the resulting Si-O-Si dimer produce the

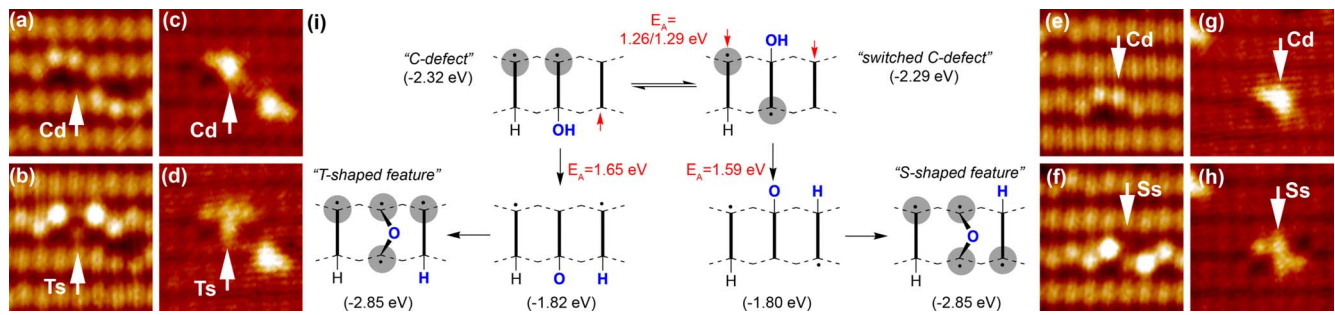


FIG. 4. (Color online) STM image sequences showing additional transformations of *C* defects (labeled Cd): [(a)–(d)] The sequence on the right-hand side shows the formation of a T-shaped feature (labeled Ts). [(e)–(h)] On the left-hand side, an S-shaped feature (Ss) is formed. The proposed reaction mechanism is shown in the center (i): OH dissociation by interdimer H shift to a third dimer, commencing with regular and switched *C* defects, produces T- and S-shaped features, respectively. Imaging threefold bonded silicon sites are shaded in gray.

double-dot protrusion seen in the STM images [white arrow in Figs. 3(e) and 3(f)]; the adjacent monohydride dimer exhibits a hallmark dark-dimer appearance. These assignments are consistent with the Tersoff–Hamann simulated STM images.¹⁹ An illustrative image simulation is included for the double-dot feature as the insets of Figs. 3(e) and 3(f).

The STM assignments are compelling in light of the calculated energetics [Fig. 3(g)]. Transitions between regular and switched *C* defects occur very frequently (every few STM frames) and proceed in both directions. The calculations explain why the two structures are of near equal formation energy (–2.32 vs –2.29) and the activation energies for OH switching (1.29 and 1.26 eV, respectively) are readily accessible at 450 K. In contrast, the onward reaction to the double-dot feature occurs only sporadically over several hours of imaging. This is explained by the much higher barrier (1.54 eV) for OH dissociation by interdimer H shift. The intermediate oxygen adatom species is short lived (and not seen by STM) due to the low activation barrier (0.37 eV) for the insertion of oxygen into the Si-Si dimer.²⁰ An overall 0.7 eV energy gain relative to the *C* defect ensures that the reverse reaction from double dot to *C* defect cannot occur, which is in agreement with observation.

The two-dimer double-dot feature also has two companion features that are *three* dimers wide. Pairs of images in Figs. 4(a)–4(d) and Figs. 4(e)–4(h) show *C* defects converting into a T-shaped (Ts) and an S-shaped feature (Ss), respectively. Both features are composed in filled state [Figs. 4(b) and 4(f)] of a bright protrusion on the outer dimers and a somewhat darker dimer in the center. The reaction diagram in Fig. 4(i) explains how these features come about. As for the double-dot feature, the formation starts out with the rapidly reversing OH-switch reaction between regular and switched *C* defects, with OH dissociation by interdimer H shift again being the rate-determining step. Depending on the switching state of the *C* defect and the direction of the H shift, the hydrogen atom may be transferred to one of three sites (indicated by red arrows). One of these sites produces a monohydride and hence the double-dot feature as described above, while the other two possibilities result in the S- and T-shaped features. The H-shift activation barriers leading to double-dot, S-shaped, and T-shaped features are very similar (1.54, 1.59, and 1.65 eV, respectively), which are consistent

with the formation of all three features at 450 K. We note in passing that the same-dimer H+OH species (the asymmetric feature in Figs. 1 and 2) is seen to undergo dissociation in isolated instances. Preliminary analysis suggests that OH dissociation by interdimer H shift is also the governing process for the same-dimer H+OH dissociation with a calculated barrier of 1.78 eV. This relatively high barrier is consistent with its low likelihood experimentally at 450 K.

We are now in a position to comment on the missing link between room-temperature water adsorption and the single-dimer H-Si-O-Si-H motif observed at 575–675 K.³ Critically, dimer-to-dimer diffusion of hydrogen atoms is activated in this temperature range.^{21,22} As we have shown, the *C*-defect dissociation processes at 450 K produce surface-inserted oxygen atoms with two hydrogen atoms variously distributed on surrounding dimers. For the case of the double-dot feature, Fig. 5 outlines how the two hydrogen-diffusion reactions result in the single-dimer H-Si-O-Si-H species. At –3.52 eV, this species is much more stable than the double-dot precursor (–3.01 eV); thus, we would expect H-Si-O-Si-H to form as soon as the relevant H-diffusion barriers (1.69 and 1.94 eV) become thermally activated. Analogous processes apply to S- and T-shaped features. Overall, the adsorption of H₂O and the subsequent steps of dissociation, incorporation, and recombination lead to structures of increasingly lower energy.

In summary, a combination of STM experiments conducted at elevated temperatures, guided by DFT reaction path calculations, provides direct images of the water-

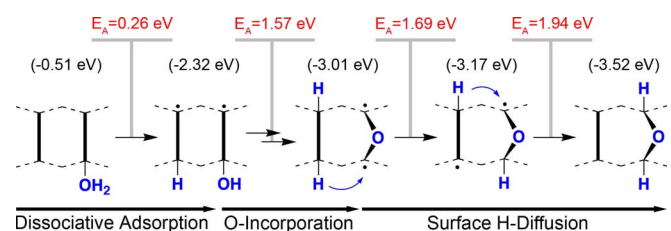


FIG. 5. (Color online) Outline illustration of temperature activated processes leading to the formation of the single-dimer H-Si-O-Si-H species via a series of intermediate species of increasing energetic stability. For each of the transitions shown, the rate-determining activation energies (E_A) are given.

induced silicon surface oxidation. This leads to the identification of a number of important intermediate species and elucidates OH dissociation by interdimer H shift as a key elementary reaction step. Knowledge of these fundamental processes provides essential new input for large-scale models such as kinetic Monte Carlo (e.g., Ref. 14) used to describe the collective processes of wet silicon surface oxidation.

This work was supported by the Australian Research Council, the Australian Government, the Australian Partnership for Advanced Computing, and the U.S. Advanced Research and Development Activity, National Security Agency, and Army Research Office under Contract No. DAAD19-01-1-0653. S.R.S. is supported by the Australian Research Council (No. DP0557331).

-
- ¹Y. J. Chabal, *Phys. Rev. B* **29**, 3677 (1984).
²M. Chander, Y. Z. Li, J. C. Patrin, and J. H. Weaver, *Phys. Rev. B* **48**, 2493 (1993).
³M. K. Weldon, B. B. Stefanov, K. Raghavachari, and Y. J. Chabal, *Phys. Rev. Lett.* **79**, 2851 (1997).
⁴M. Z. Hossain, Y. Yamashita, K. Mukai, and J. Yoshinobu, *Phys. Rev. B* **67**, 153307 (2003).
⁵S. Okano and A. Oshiyama, *Surf. Sci.* **554**, 272 (2004).
⁶J.-Y. Lee and J.-H. Cho, *J. Phys. Chem. B* **110**, 18455 (2006).
⁷S. Carniato, J. J. Gallet, F. Rochet, G. Dufour, F. Bournel, S. Rangan, A. Verdini, and L. Floreano, *Phys. Rev. B* **76**, 085321 (2007).
⁸S.-Y. Yu, H. Kim, and J.-Y. Koo, *Phys. Rev. Lett.* **100**, 036107 (2008).
⁹R. J. Hamers and U. K. Köhler, *J. Vac. Sci. Technol. A* **7**, 2854 (1989).
¹⁰B. R. Trenhaile, A. Agrawal, and J. H. Weaver, *Appl. Phys. Lett.* **89**, 151917 (2006).
¹¹H. Watanabe, S. Nanbu, Z.-H. Wang, and M. Aoyagi, *Chem. Phys. Lett.* **424**, 133 (2006).
¹²B. B. Stefanov and K. Raghavachari, *Appl. Phys. Lett.* **73**, 824 (1998).
¹³Y. Okamoto, *Phys. Rev. B* **60**, 10632 (1999).
¹⁴A. Esteve, Y. J. Chabal, K. Raghavachari, M. K. Weldon, K. T. Queeney, and M. Djafari Rouhani, *J. Appl. Phys.* **90**, 6000 (2001).
¹⁵M. J. Frisch *et al.*, GAUSSIAN03, Revision C.02 (Gaussian, Inc., Wallingford CT, 2004).
¹⁶We use a composite Gaussian-type basis set [6-311++G(*d,p*) for adsorbate and surface-dimer atoms; 6-311G(*d,p*) for second row atoms and LANL2DZ for all other atoms]. Two energy corrections were applied to estimate the effect of extending cluster size and basis set to four-dimer Si₅₃H₄₄ and 6-311++G(2*df*,2*pd*), respectively [details in O. Warschkow, T. L. McDonnell, and N. A. Marks, *Surf. Sci.* **601**, 3020 (2007)]. Frequency calculations were performed to supply vibrational zero-point energies and to distinguish true minima and transition states. Energies are given relative to a gas-phase molecule and the free surface cluster.
¹⁷K. Hata, S. Ozawa, and H. Shigekawa, *Surf. Sci.* **441**, 140 (1999).
¹⁸The clean Si surface was prepared by degassing followed by direct current annealing to 1400 K to remove the oxide layer. Water was purified through freeze-pump-thaw cycles and introduced to the chamber via a leak valve.
¹⁹Simulated empty- and filled-state STM images were produced in the Tersoff–Hamann approximation [J. Tersoff and D. R. Hamann, *Phys. Rev. Lett.* **50**, 1998 (1983)] tracing the $2.7 \times 10^{-4} e/\text{\AA}^3$ isosurface of the integrated local density of state (ILDOS) over a 1 V interval above and below the Fermi level, respectively. The ILDOS was calculated using a plane-wave-pseudopotential DFT model and a four-layer silicon slab model of 4×4 surface periodicity; for calculational details, see, S. R. Schofield, S. A. Sarairoh, P. V. Smith, M. W. Radny, and B. V. King, *J. Am. Chem. Soc.* **129**, 11402 (2007).
²⁰The alternative insertion of oxygen into a Si-Si backbond is not observed. With a calculated activation barrier of 1.22 eV, backbond insertion cannot compete with dimer-bond insertion.
²¹J. H. G. Owen, D. R. Bowler, C. M. Goringe, K. Miki, and G. A. D. Briggs, *Phys. Rev. B* **54**, 14153 (1996).
²²E. Hill, B. Freelon, and E. Ganz, *Phys. Rev. B* **60**, 15896 (1999).